Constant Envelope Fractional Fourier Transform based Waveform Libraries for MIMO Radar

Christos V. Ilioudis *, Carmine Clemente*, Ian Proudler†, John J. Soraghan*
*Centre for Excellence in Signal and Image Processing, University of Strathclyde, Glasgow, United Kingdom
Email: c.ilioudis@strath.ac.uk, carmine.clemente@strath.ac.uk, j.soraghan@strath.ac.uk
† School of Electronic, Electrical and Systems Engineering, Loughborough University, Leicestershire, UK
Email: i.k.proudler@lboro.ac.uk

***Abstract*—In this paper an efficient technique to generate novel libraries of phase-coded waveforms with constant envelope aimed at optimizing signal retrieval is presented. The modulation technique is based on the Fractional Fourier Transform (FrFT), where the signal waveforms retain their constant modulus. Reconstruction of sequences from the FrFT based waveforms is explored by means of the Error Reduction Algorithm (ERA), while the constant envelope property is kept unchanged. Additionally comparison between reconstructed and original sequences is also carried out in terms of performance and cross-correlation properties of the signals. Simulation results demonstrate the effectiveness of the novel waveform libraries considering design parameters such as resolution, interfering power, orthogonality and signal bandwidth.**

Keywords: Fractional Fourier Transform (FrFT); Constant Envelope (CE); Fractional Waveform Libraries; Error Reduction Algorithm (ERA).

I. Introduction

Recently radar applications such as target detection and tracking are getting higher attention and becoming more demanding, providing further challenges to the signal processing research community. Among these challenges, waveform design plays an important role, especially for applications in electromagnetically crowded scenarios and where covertness is required. Driven by the beneficial implementation of DSP technology, signal waveform designs have been improved allowing remarkable increase in detection, tracking and classification performance. As modern radar systems are increasingly being required to operate in continuously altering and overcrowded electromagnetic environments, their effective operation can be restricted due to severe interference mitigation, frequency occupancy, security, and performance constraints [1]. In the presence of these difficulties, the selection of robust waveform design that allows good Doppler resolution, short delays, high signal energy using low peak power and high spectrum efficiency poses a major challenge. Good spectral efficient waveforms are an essential component in modern radar imaging systems [2]. Several design methods based on fixed and adaptive radar waveforms have been extensively investigated providing waveforms suitable for different applications in [3], [4] and [5]. However most proposed designs involve an adjustment between some of their characteristics such as range resolution versus side lobe levels (SLL) [1], [2].

Recently we proposed a new approach for producing radar waveform libraries using the fractional Fourier Transform (FrFT) [6]. These novel libraries were shown to provide significant advantages in terms of delay resolution, interference and side lobe level reduction. Increased performance is shown in terms of orthogonality and reuse of waveform for the same canonical sequence (e.g. Barker 13) but with different fractional orders when higher values of chip sampling rate are used [7]. Despite the fact that FrFT based waveforms libraries offer good properties, unlike the original classical sequences (Barker 13, Frank, P4, etc.), they do not preserve constant envelope (CE) property. Constant modulus or Peak-to-Average Power Ratio (PAPR) is an essential characteristic for real world applications, as radar signal amplifiers usually work in a saturation condition that maximizes their efficiency but preventing amplitude modulation in waveforms at the same time. In [8] two optimisation algorithms were introduced for maximizing the Signal to Interference plus Noise Ratio (SINR) in a collocated MIMO radar system taking into account constant modulus and similarity constrains. Both algorithms have been showed good performance trading however with hight complexity.

In this paper a new technique that uses FrFT phase coded waveforms to achieve constant modulus by means of the error-reduction or Gerchberg-Saxton algorithm (GSA) [9] is presented. Furthermore Zadoff-Chu sequences [10] are used as a starting point in the algorithm given their constant modulus and good autocorrelation properties. The generated waveforms are validated based on their ambiguity function (AF) extracting important characteristics such as delay, Doppler resolutions, side lobes, bandwidth, interference and interference power ratio. An analysis of the cross-interference and waveform reuse is also presented. Finally simulation results are presented to demonstrate the effectiveness of the new technique and the abilities of the proposed new waveform libraries.

The remainder of the paper is organized as follows. Section II introduces the fractional Fourier transform and a formulation of the constant amplitude problem. The Error Reduction Algorithm is presented in Section III as a mean of generating the FrFT based constant amplitude waveform libraries. Results and performance analysis are presented in Section IV for a sample of novel waveform libraries while Section V concludes the paper.

II. Problem Formulation

A. Fractional Fourier Tranform (FrFT) based Waveforms

Fractional Fourier transforms (FrFTs) belong to the class of linear time-frequency representations (TFRs) firstly introduced by Namias in 1980 [11]. The FrFT transforms a function

978-1-4799-5294-6/14/$31.00 ©2014 IEEE

to any intermediate domain between time and frequency. To compute FrFT the angle of axis rotation, θ, is used in the time-frequency plane as the fractional power of the ordinary Fourier transform. It has been used in a wide rage of applications such as waveform propagation, filter design, signal analysis and pattern recognition. Letting $x[u']$ be an arbitrary signal of length U, its a^{th}-order discrete FrFT is defined as [12]:

$$FrFT_a\big[x[u]\big] = \mathbf{X}_a[u] = \sum_{u'=-U/2}^{U/2} K_a[u,u']x[u'] \quad (1)$$

where a is the fractional transformation order (corresponding to a rotation angle $\theta = a\frac{\pi}{2}$ with $a \in \mathcal{R}$) and $K_a[u,u']$ is the FrFT kernel defined as [12]:

$$K_a[u,u'] = \begin{cases} A_0 \exp\{j\pi[(u^2+u'^2)\cot\theta - 2uu'\csc\theta]\} \\ \text{if } \theta \text{ is not a multiple of } \pi \\ \delta[u-u'] \text{ if } \theta \text{ is a multiple of } 2\pi \\ \delta[u+u'] \text{ if } \theta+\pi \text{ is a multiple of } 2\pi \end{cases} \quad (2)$$

where $\delta(.)$ is the Dirac delta function, $A_0 = \frac{e^{j\frac{\theta}{2}}}{\sqrt{j\sin\theta}}$ and $j = \sqrt{-1}$.
The FrFT is an invertible linear transform, continuous in the angle θ, which satisfies the basic conditions for it to be meaningful as a rotation in the time-frequency plane.

The FrFT can be applied to common waveforms, such as phase-modulated waveforms with different codes (e.g. Barker or P4 codes) [6] ,[7] . Let $s[n[$ represent a canonical waveform (e.g. the traditional Barker 13 code) from which the Fractional Fourier transform library elements, $\mathbf{S}_{a_i}[u]$ with $i = 1, ..., L$ are obtained by applying (1). Thus a fractional waveform library is defined as:

$$\mathbf{S} = [S_{a_1}[u], S_{a_2}[u], \ldots, S_{a_L}[u]] \quad (3)$$

where $a_i \in [0,1]$, and L represents the total number of waveforms populating the library. Note that for $a_i = 0$ the corresponding rotation angle $\theta = 0$, resulting in the canonical waveform. The value of L depends on several aspects such as the original waveform used, waveform reuse, orthogonality requirements and applications.

An analytical representation of each fractional library element requires the cardinality of the waveform Ω (i.e. the number of chips used in a code sequence) and the number of samples per chip r to be introduced. The total digital signal length is obtained as: $N = \Omega \times r$, denoting the total number of waveform samples. Defining $\mathbf{c} = [c_1, c_2, \ldots, c_N]$ as the vector of N samples for the original waveform, the resulting canonical waveform, $s[n]$, can be expressed as:

$$s[n] = \sum_{k=1}^{N} c_k \delta[n-k] \quad (4)$$

Now applying the FrFT to (4) and using the properties presented in [13] the set of fractional library elements can be written as:

$$S_a[u] = \sum_{k=1}^{N} c_k FrFT_a[\delta[n-k]] = \sqrt{\frac{1-j\cot\theta}{2\pi}} \sum_{k=1}^{N} c_k e^{j\frac{k^2+u^2}{2}\cot\theta - juk\csc\theta} \quad (5)$$

where $FrFT_a[.]$ represents the Fractional Fourier Transform of the a^{th} order as defined in (1) and (2).

From (5) the l^{th}-element of $\mathbf{S}$ is the sum of N chirped functions weighted by the original waveform sequence with a modulation rate that depends on a and k. Since the number of chirped components depends on N, and this is the product of the code cardinality and the chip sampling rate r, different waveforms can be obtained from a given canonical waveform by changing r.

B. Constant Envelope

For a better understanding of the Constant Envelope constraint let $y[u]$ be an arbitrary waveform. The vector $y[u]$ can be represented as:

$$y[u] = |y[u]|e^{j\eta[u]} \quad (6)$$

where $|.|$ denotes the absolute value and $\eta(u)$ is the phase of the waveform. For $y[u]$ the requirement of Constant Envelope (CE) means that its amplitude must be kept constant for all u, which is equivalent to:

$$|y[u]| = A, \quad \forall u \quad (7)$$

where A is a suitable positive constant that can be also used to sustain the energy of $y[u]$ at a desired level [14].

Typically in current power amplifiers high linearity implies low power efficiency and vice-versa [15]. This low efficiency operation is due to the fact that the amplifying device must be biased to an average output power level low enough to accommodate peak input signal levels without over-driving the amplifying device. Therefore linearity requirement can be met by driving the power amplifier well below its saturation point. To achieve better performance the use of non-linear components is required. Non-linear power amplifiers preserve only phase and no amplitude information. The previous work describing the use of the FrFT to form libraries of useful waveforms did not satisfy the CE constraint [7], [6]. In this particular case the CE constrain problem can be described as finding waveforms with constant modulus that also have similar behaviour to the FrFT modulated waveforms.

III. Error-Reduction Algorithm

The error-reduction or Gerchberg-Saxton algorithm (GSA) was first introduced in connection with the problem of reconstructing phase from two intensity measurements [16]. The algorithm can be described by the following simple four steps [9]: (1) Fourier transform an estimate of the reference sequence; (2) replace the modulus of the resulting computed Fourier transform with the reference Fourier modulus to form an estimate of the Fourier transform; (3) inverse Fourier transform the estimate of the Fourier transform; and (4) replace the modulus of the resulted computed sequence with the reference sequence modulus to form a new estimate of the reference sequence. In a more general definition GSA transforms back and forth between the frequency and time domain, satisfying the constraints in one before returning to the other resulting to decreased error at each iteration.

For this particular case the reference sequence is a non-CE fractional Fourier modulated waveform $S_a(u)$ and $g_k(u)$ is a CE sequence which iterates closer to $S_a(u)$ in every execution of the GSA loop. Zadoff-Chu [10] sequences are

chosen as starting point of GSA due to its faster and better performance compared to random initial seeds according to the results presented in [17]. To generate Zadoff-Chu sequences a modified formula is implemented that supports both odd and even sequence lengths [18]. Additionally to apply the CE constrain on the new waveforms the modulus of the referenced sequence has been replaced with a constant, A, in the fourth step of GSA. The k^{th} loop of this modified version of GSA can be described by the following four steps:

$$G_k[f] = |G_k[f]|e^{j\phi_k[f]} = \mathcal{F}\big[g_k[u]\big], \tag{8}$$

$$G'_k[f] = |\hat{S}_a[f]|e^{j\phi_k(f)} = |\mathcal{F}\big[S_a[u]\big]|e^{j\phi_k[f]} \tag{9}$$

$$g'_k[u] = |g'_k[u]|e^{j\psi'_k[u]} = \mathcal{F}^{-1}\big[G'_k[f]\big], \tag{10}$$

$$g_{k+1}[u] = Ae^{j\psi k+1(u)} = Ae^{j\psi'_k[u]} \tag{11}$$

where $\mathcal{F}[.]$ is the Fourier transform and, ϕ_k and ψ_k are the phases in time and frequency domain of $g_k[u]$. A graphical representation of the algorithm is provided in Fig. 1 where the modified GSA loops are repeated.

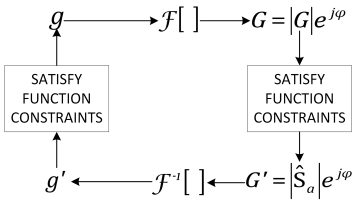

Fig. 1. Block diagram of the Gerchberg-Saxton algorithm.

IV. Simulation Results: Analysis and Evaluation

In the following subsections a detailed performance analysis of two example novel libraries is presented. Generated libraries for the conventional Barker 13 and P4 25 codes [1] are analysed in terms of PAPR, AF performance parameters and orthogonality for varying fractional order a and different chip sampling rates r.

A. Analysis Framework

To verify the CE constraint the PAPR of the both constant and non-constant envelope waveforms are evaluated for altering fractional orders and different chip sampling rates. Additionally to quantify the effectiveness of the novel libraries various AF performance parameters are examined using the following:

- Delay and Doppler resolution, computed as the -3 dB width of the zero-Doppler and zero-delay cut of the ambiguity function respectively;
- Delay and Doppler side lobe level, computed as the level of the first side lobe of the zero-Doppler and zero-delay cut of the ambiguity function respectively;
- Modulated signal bandwidth, computed as the -3 dB width of the transmitted signal spectrum;
- Interfering power, computed as the power outside the main lobe;
- Interfering power ratio, computed as the ratio between the power in the side lobes of the ambiguity function and main lobe power.

In the presented analysis, constant envelope fractional waveforms are compared with their originals in terms of the performance parameters defined above. By definition better performance results for smaller values of all parameters. Orthogonality properties of a library are evaluated assuming that both waveforms $S_{a_i}(u)$ and $S_{a_j}(u)$ are generated from the same conventional sequence $\mathbf{c}$ but using different fractional order, $a_i \neq a_j$. We define that $S_{a_i}(u)$ and $S_{a_j}(u)$ are orthogonal if their cross-correlation is below the side-lobe level (SLL) of original sequence $\mathbf{c}$. In the present analysis canonical Barker 13 and P4-25 are used as original sequences with SSL -22.18 dB and -22.22 dB respectively.

B. Results

The performance parameters and waveform reuse are evaluated for the Barker 13 and P4 25 canonical sequences using 50 and 200 samples per chip. Specifically the PAPR of the fractional libraries is illustrated in Fig. 2. As it can be seen the non-CE waveforms tend to have higher peak-to-average power ratio as the fractional order increases for both canonical sequences. On the other hand the CE waveforms have unity PAPR for all fractional orders which confirms the CE constraint. In both cases the sampling rate r does not have any significant impact.

The performance and orthogonality of CE and non-CE FrFT modulated Barker 13 code are compared in Fig. 3 using $r = 50$. Figure. 3(a) shows that delay resolution is identical for both cases, while Doppler resolution is improved for higher fractional orders after using the CE constraint. Figure 3(b) demonstrates that delay and Doppler sidelobes have the same behaviour for both CE and non-CE waveforms. Additionally interference and interference power ratio perform similarly for both cases as it is shown in Fig. 3(c). The orthogonality map presented in Fig. 3(d) indicate the poor reuse of the CE waveforms as wide continuous black blocks (above SSL threshold) correspond to high reuse interval compared to non-CE [7].

Similarly to Fig. 3, Fig. 4 illustrates the performance and orthogonality using $r = 200$. It can be observed that after increasing r the performance of CE and non-CE waveforms has been increased similarly in terms of resolution and sidelobes. Also interference and interference power ratio have been decreased, for both cases with CE waveform performing better at high fractional orders.

To compare different canonical sequences, simulations are repeated using P4 25 code sequence for both cases of $r = 50$ and $r = 200$ samples per chip. Results presented in Fig. 5 and Fig. 6 indicate similar behaviour in terms of performance to Barker 13 code for both CE and non-CE waveforms. On the other hand P4 25 code sequence performs better than Barker 13 one in terms of orthogonality and waveform reuse both for low and high values of r.

Table I summarizes maxima (worst cases) of the reuse intervals extracted for both CE and non-CE fractional libraries. The reuse intervals are estimated for each value of a by measuring the gaps in terms of fractional orders between the used $S_{a_i}[u]$ and the first $S_{a_j}[u]$ with a cross-correlation maximum with $S_{a_i}[u]$ below the threshold. As it can be seen CE libraries present higher reuse intervals for small values of r compared to the non-CE. However both CE and non-CE libraries have significantly lower reuse interval

for higher values of r. This results to a higher reuse as the number of orthogonal waveforms in the same library is given by the ratio of the available fractional order interval ($\max(a) = 1$ due to symmetry of FrFT) to their maximum reuse interval. Specifically up to eight orthogonal waveforms can be obtained in the case of P4 25 with $r = 200$ (i.e. $1/0.12 \simeq 8$). This number can be increased by limiting the values of fractional order to ranges of lower reuse interval. Figure 7 illustrates the case in which the fractional order a has been limited to values between 0.13 and 1 decreasing maximum to 0.02 and constituently resulting more than 40 (i.e. $0.87/0.02 \simeq 43$) orthogonal waveforms available. It is worth noting that different seed sequences (i.e. starting points in GSA) are used for each individual fractional order in simulation examples. This is achieved by changing the root of Zadoff-Chu sequences [18].

Finally no considerable improvement or declination was observed in terms of bandwidth usage after the modulation in any simulation.

TABLE I. FRACTIONAL ORDER REUSE INTERVAL FOR DIFFERENT VALUES OF r

Sequence	Constant Envelope		non-Constant Envelope	
	$r = 50$	$r = 200$	$r = 50$	$r = 200$
Barker 13	1.43	0.21	0.77	0.22
P4 25	0.4	0.12	0.49	0.12

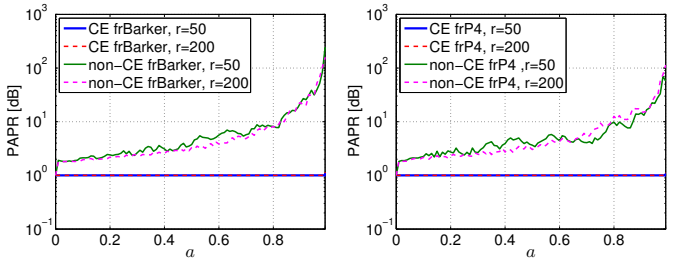

(a) frBarker (b) frP4

Fig. 2. Peak-to-Average Power Ratio (PARP) of CE and non-CE Barker 13 (a) and P4 25 (b) fractional waveforms of different fractional order using $r = 50$ and $r = 200$.

V. CONCLUSIONS

In this paper the design of novel waveform libraries is addressed by a method based on the Fractional Fourier Transform (FrFT) and the Error Reduction Algorithm (ERA). Reconstruction of fractional waveforms is achieved by means phase retrieval applying the Gerchberg-Saxton algorithm (GSA) to retain the Constant Envelope (CE) property. The main design algorithms are examined and implemented to generate novel fractional waveform libraries having improved properties with regard to resolution, interfering power, orthogonality and signal bandwidth.

A constructive technique for numerical estimation of CE waveforms is described and illustrated on several waveform simulation examples. The performance of the new waveform library is evaluated as a function of the FrFT order and chip sampling rate. The results illustrate cases where waveforms can keep their constant envelope property after transformation for low and high values of samples per chip using two phased coded sequences (Barker 13 and P4 25). Future research will be focused on down-sampling CE FrFT modulated waveforms with high values of r and evaluate their performance and reuse.

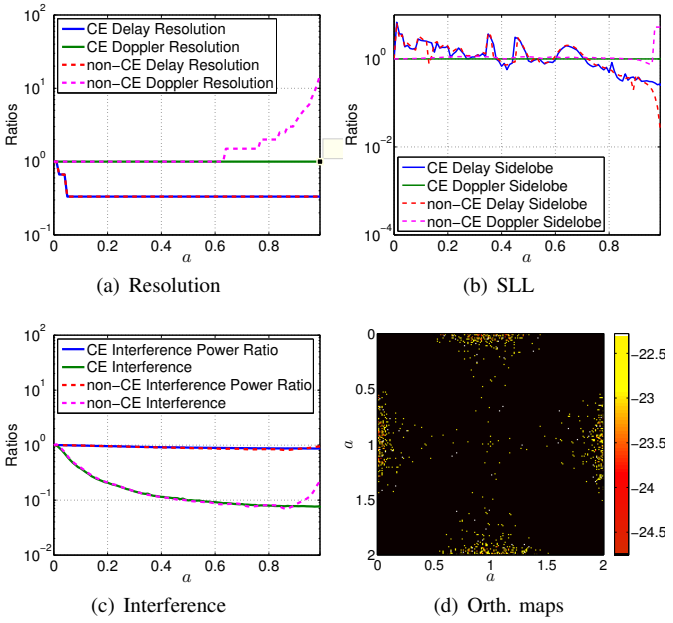

(a) Resolution (b) SLL

(c) Interference (d) Orth. maps

Fig. 3. Ratios of the AF quality parameter for fractional Barker 13 waveforms of different a before and after applying CE constraints in terms of resolution (a), side lobe level (b) and interference (c), and SLL-thresholded maxima (cases above the thresholds are shown in black) of the cross-correlations between CE fractional Barker 13 waveforms of different a and different GSA starting points (d), for $r = 50$.

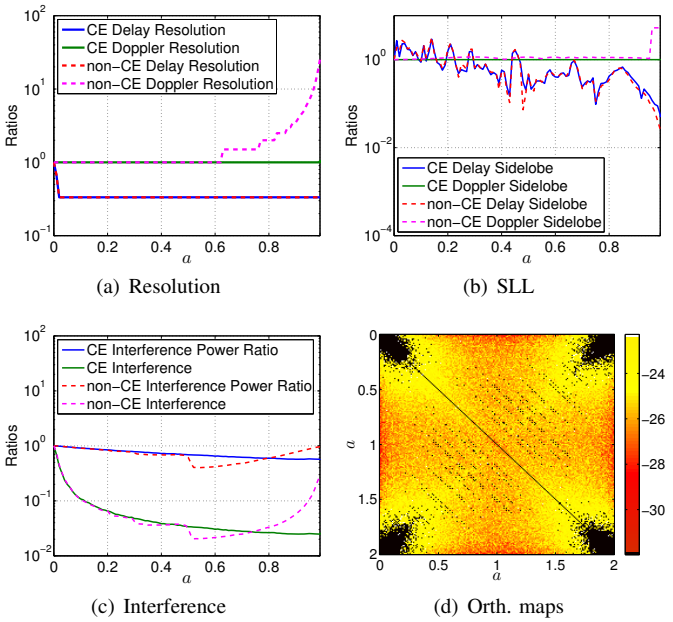

(a) Resolution (b) SLL

(c) Interference (d) Orth. maps

Fig. 4. Ratios of the AF quality parameter for fractional Barker 13 waveforms of different a before and after applying CE constraints in terms of resolution (a), side lobe level (b) and interference (c), and SLL-thresholded maxima (cases above the thresholds are shown in black) of the cross-correlations between CE fractional Barker 13 waveforms of different a and different GSA starting points (d), for $r = 200$.

ACKNOWLEDGMENT

This work was supported by the Engineering and Physical Sciences Research Council (EPSRC) Grant number EP/K014307/1 and the MOD University Defence Research Collaboration in Signal Processing.

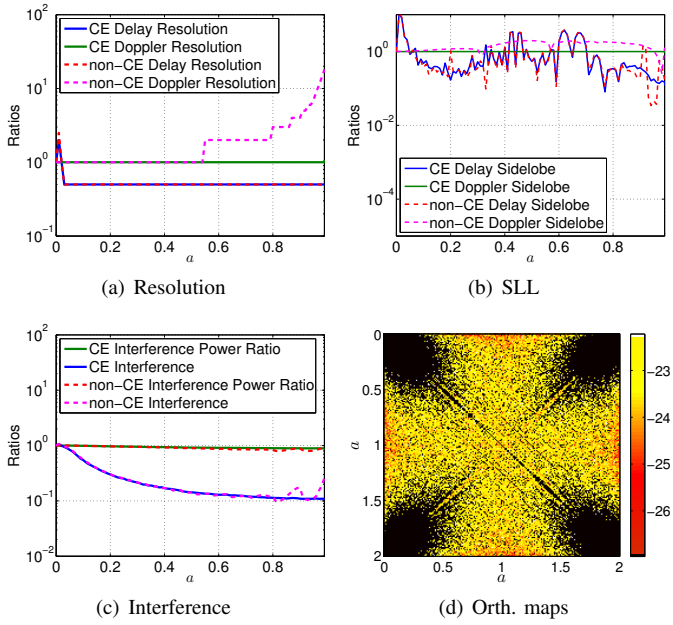

(a) Resolution (b) SLL

(c) Interference (d) Orth. maps

Fig. 5. Ratios of the AF quality parameter for fractional P4 25 waveforms of different a before and after applying CE constraints in terms of resolution (a), side lobe level (b) and interference (c), and SLL-thresholded maxima (cases above the thresholds are shown in black) of the cross-correlations between CE fractional P4 25 waveforms of different a and different GSA starting points (d), for $r = 50$.

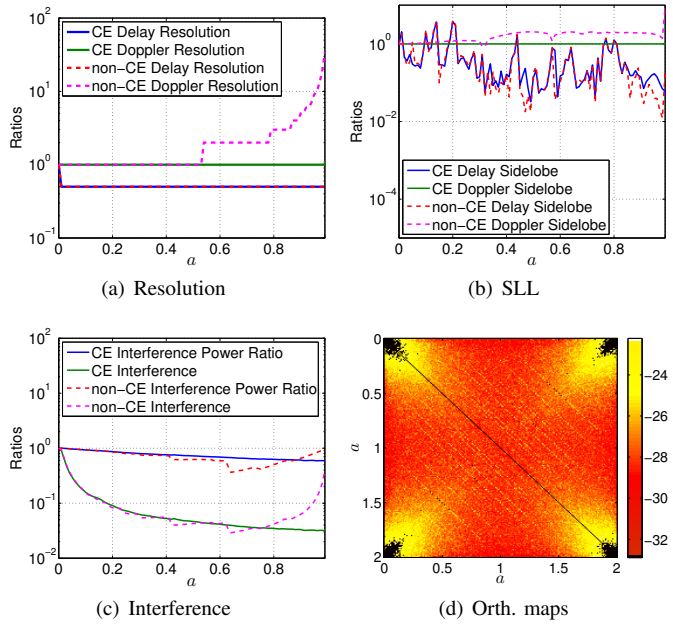

(a) Resolution (b) SLL

(c) Interference (d) Orth. maps

Fig. 6. Ratios of the AF quality parameter for fractional P4 25 waveforms of different a before and after applying CE constraints in terms of resolution (a), side lobe level (b) and interference (c), and SLL-thresholded maxima (cases above the thresholds are shown in black) of the cross-correlations between CE fractional P4 25 waveforms of different a and different GSA starting points (d), for $r = 200$.

REFERENCES

[1] N. Levanon and E. Mozeson, *Radar Signals*, NY: JohnWiley & Sons, 2004.

[2] F. Gini, A. De Maio, and L. Patton, *Waveform Design and Diversity for Advanced Radar Systems*, IET radar, sonar and navigation series. Institution of Engineering and Technology, 2012.

[3] Ruixin Niu, P. Willett, and Y. Bar-Shalom, "Tracking considerations in selection of radar waveform for range and range-rate measurements," *Aerospace and Electronic Systems, IEEE Transactions on*, vol. 38, no. 2, pp. 467–487, Apr 2002.

[4] Constantino Rago, P. Willett, and Y. Bar-Shalom, "Detection-tracking performance with combined waveforms," *Aerospace and Electronic Systems, IEEE Transactions on*, vol. 34, no. 2, pp. 612–624, Apr 1998.

[5] C.R. Berger, B. Demissie, J. Heckenbach, P. Willett, and Shengli Zhou, "Signal Processing for Passive Radar Using OFDM Waveforms," *Selected Topics in Signal Processing, IEEE Journal of*, vol. 4, no. 1, pp. 226–238, Feb 2010.

[6] C. Clemente, I. Shorokhov, I. Proudler, and J. Soraghan, "Radar Waveform Libraries Using Fractional Fourier Transform," in *2014 IEEE Radar Conference, Cincinnati, Ohio, 19-23 May 2014*.

[7] C. Clemente, C. Ilioudis, D. Gaglione, K. Thompson, S. Weiss, I. Proudler, and J. Soraghan, "Reuse of Fractional Waveform Libraries for MIMO Radar and Electronic Countermeasures," in *6th International Symposium on Communications, Control, and Signal Processing (ISCCSP 2014), Athens, Greece, 21-23 May 2014*.

[8] Guolong Cui, Hongbin Li, and M. Rangaswamy, "MIMO Radar Waveform Design With Constant Modulus and Similarity Constraints," *Signal Processing, IEEE Transactions on*, vol. 62, no. 2, pp. 343–353, Jan 2014.

[9] J. R. Fienup, "Phase retrieval algorithms: a comparison," *Applied optics*, vol. 21, no. 15, pp. 2758–2769, 1982.

[10] R. Frank, S. Zadoff, and R. Heimiller, "Phase shift pulse codes with good periodic correlation properties (Corresp.)," *Information Theory, IRE Transactions on*, vol. 8, no. 6, pp. 381–382, October 1962.

[11] V. Namias, "The fractional order Fourier transform and its application to quantum mechanics.," *Journal of Institute of Mathematics and its Applications*, pp. 241–265, 1980.

[12] H. M. Ozaktas, Z. Zalevsky, and M. A. Kutay, *The Fractional Fourier Transform with applications in Optics and Signal Processing*, John Wiley & Sons Ltd, UK, January 2001.

[13] L. B. Almeida, "The fractional Fourier Transform and time-frequency representations," *IEEE Transactions on Signal Processing*, vol. 42, no. 11, pp. 3084–3091, November 1994.

[14] S.U. Pillai, Ke Yong Li, and H. Beyer, "Reconstruction of constant envelope signals with given Fourier transform magnitude," in *Radar Conference, 2009 IEEE*, May 2009, pp. 1–4.

[15] C. Cripps, S., *Advanced techniques in RF power amplifier design*, Artech House, 2002.

[16] W. Gerchberg, R. and O. Saxton, W., "A practical algorithm for the determination of the phase from image and diffraction plane pictures," in *Optik 35*, 1972, pp. 237–246.

[17] A. Santra, K. Jadia, and Alleon G. Srinivasan, R., "Generation Of Modulus Constraint Signal In Adaptive Radar Waveform," in *9th International Radar Symposium India 2013 (IRSI-13)*, December 2013.

[18] S. Budisin, "Decimation Generator of Zadoff-Chu Sequences," in *Sequences and Their Applications - SETA 2010,6th International Conference*, C. Carlet and A. Pott, Eds.

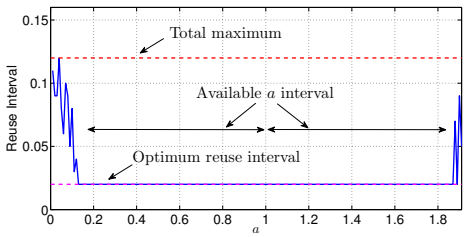

Fig. 7. Reuse interval of CE fractional P4 25 waveforms of different a for $r = 200$ and its overall and optimum maxima resulting for different interval of a.